Microjet Printing of Micro-optical Interconnects and Sensors

W. Royall Cox*, Chi Guan and Donald J. Hayes
MicroFab Technologies, Inc., 1104 Summit Ave., Suite 110, Plano, TX 75074

ABSTRACT

The microjet printing method is being used to fabricate microlens arrays for use in massively parallel, VCSEL-based datacom switches and to deposit lenslets of various configurations onto the tips of single-mode telecom fibers. Applications in the latter case include collimation of the output beams for free space optical interconnection and increasing the fiber numerical aperture for collection of light from edge-emitting diode lasers. Additional applications of this technology include printing of arrays of active sensor elements onto the tips of imaging fiber bundles and fabrication of microlenses with axial index of refraction gradients to reduce focal spot size, utilizing multiple print heads with differing fluids. This low-cost, data-driven process, based on "drop-on-demand" inkjet technology, involves the dispensing and placing of precisely sized microdroplets of optical material onto optical substrates. The micro-optical elements are printed with 100% solid, UV-curing optical epoxies, utilizing printing devices that can dispense picoliter-volume droplets at temperatures up to 300°C.

Key Words: microjet printing, micro-optics fabrication, optical fibers, optical sensors

1. INTRODUCTION

The continuing advance of information transmission and processing systems of greater speed and parallelism will increasingly rely on lower-cost, higher-performance optical interconnect technologies to integrate efficiently and cost-effectively the various components in optical systems. To meet this need, an evolution in micro-optical interconnect technologies has been occurring in which organic optical materials are being widely accepted and used in the fabrication of micro-optical elements, which, in turn, has fueled the emergence of new micro-optics fabrication technologies. Of these new technologies, direct-write of refractive microlenses and waveguides, by microjet printing[1,2] or syringe dispensing,[3] has attracted increasing interest because of its: (a) data-driven flexibility; (b) low cost (single-step); (c) capability for utilization of optical epoxies with higher thermal durability than the PMMA photo-resist used in photolithographic methods;[4] and (d) unique capabilities for fabrication of micro-optical elements directly onto optical components of arbitrary geometry.[5,6]

After reviewing briefly the processes and materials used for ink-jet printing of micro-optics we will discuss firstly, utilization of this “Optics-Jet” technology in printing refractive microlenses into arrays for use in massively parallel, smart pixel-based datacom switches and onto the tips of optical fibers for telecom devices. Secondly, we will introduce two new applications of the technology, namely, the printing of indicator-chemistry elements in arrays onto the tips of fiber-optic imaging bundles for multi-functional biochemical sensors and the printing of GRIN (gradient index of refraction) microlenses for reduction of focal spot size.

2. MICRO-OPTICS PRINTING METHOD

In piezoelectric-based, drop-on-demand[7] (DOD) ink-jet printing systems, illustrated schematically in Figure 1, a volumetric change in the fluid within a printing device is induced by the application of a voltage pulse to a piezoelectric transducer which is coupled to the fluid. This volumetric change causes pressure/velocity transients to occur in the fluid which are directed to produce a drop from the orifice of the device. Here a voltage pulse is applied only when a drop is desired, as opposed to continuous[8] ink-jet printers where droplets are continuously produced, but directed to the target substrate only when needed by a charge and deflect method. One of the characteristics of ink-jet printing technology that makes it

* Contact Information: E-mail: rcox@microfab.com WWW.microfab.com Phone: 972-578-8076; Fax: 972-423-2438

generally attractive as a precision fluid micro-dispensing method is the repeatability of the process. The photo of Figure 2 shows a DOD device generating drops of test fluid from a device with a 50 μm orifice at 2,000 droplets per second, illuminated by an LED that was pulsed at the same frequency. With a camera exposure time of 1/2 sec, the droplet image seen here is the superposition 1,000 droplets, illustrating the spatial and temporal stability of the microjetting process.

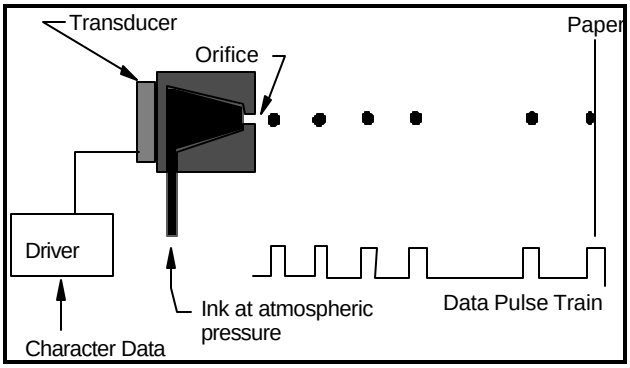

Figure 1. Drop-on-Demand ink-jet printing system.

Optical materials ranging from epoxies[9] to thermoplastics have been utilized in DOD micro-optics printing, with the most stringent requirement being the fluid formulation viscosity threshold of less than 40 cps, which is typically achieved by heating the print head to 130-175°C. The volume of a printed lenslet is a digital function of the smallest droplet size which can be generated efficiently, e.g., 20 picoliter, and its aspect ratio (diameter/sag) is determined by the degree of spreading of the deposited fluid on the target substrate prior to solidification. For UV-cured optical formulations, control of microlens aspect ratio is typically achieved by applying a low-wetting optical coating of the requisite free energy level to the substrate prior to printing and/or by heating the substrate during printing. Current hemispherical microlens printing accuracies and reproducibilities are on the order of 1% & 2% of nominal values for diameter and focal length, respectively, with relative and absolute placement accuracies of about 2 μm & 5 μm, respectively.

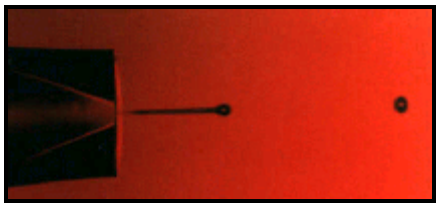

Figure 2. Generation of 50 μm droplets by DOD microjet at 2 kHz.

Refractive microlens configurations which may be microjet printed range from convex/plano hemispherical, hemi-elliptical and square,[10] to convex-convex. The latter configuration, illustrated in the photograph of Figure 3, was fabricated by printing two plano/convex lenslets coaxially on opposite sides of a 125 μm thick glass substrate. This microlens geometry, which would be more challenging to fabricate by conventional photolithographic methods, could potentially be utilized to reduce focal spot size in, e.g., optical recording applications.

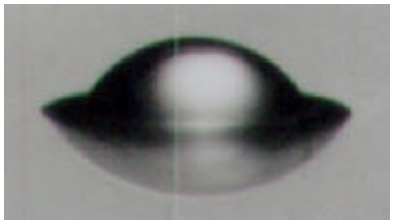

Figure 3. Two microlenses printed on opposite sides of the same substrate (top lenslet is 625 μm diameter).

3. MICROLENS ARRAYS FOR VLSI PHOTONIC SWITCH

Arrays of thousands of microlenses are being microjet printed for use as free-space optical interconnects in massively-parallel, VCSEL-based, photonic switches under development in conjunction with the DARPA VIVACE (VCSEL-based Interconnects in VLSI Architectures for Computational Enhancement) program[11]. These arrays are printed onto 3 inch diameter thin quartz wafers in 12-group patterns, where each group consists of two each 34 x 34 identical arrays of 300 μm- diameter, 60 μm-sag microlenses, giving a total of 13,872 lenslets per wafer. The microlenses in each array are printed on 500 μm centers, and the two arrays are offset from each other by 250 μm along a diagonal, such as shown in the photograph of Figure 4.

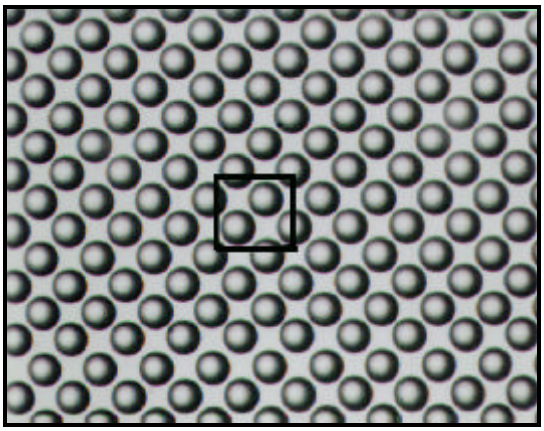

Figure 4. Portion of printed interlaced arrays of 300 μm diameter lenslets for use in "smart-pixel"-based datacom switch, where box shows two lenses within a pixel area.

The details of fabrication and functionality of this switch are beyond the scope of this paper, other than to say that a microlens-arrays is aligned to a similar VCSEL/PD array with identically interlaced patterns of vertical cavity surface emitting lasers and photodetectors, where the two lenslets within each pixel area serve to collimate the beam from a VCSEL emitter and focus a returning beam into the adjacent photodetector. Selection of printed microlenses for this application was

based on the greater coupling efficiency and wavelength independence of refractive lenslets compared to diffractive ones, the high lenslet speeds required (f/# ~ 1-2), and the greater thermal durability of optical epoxy compared to the photoresist used in photolithographically fabricated refractive lenslets.

4. MICROLENSES PRINTED ONTO TIPS OF SINGLE-MODE OPTICAL FIBERS

4.1 Increasing fiber acceptance angle

Increasing the angle of acceptance of light into an optical fiber is of interest because it can relieve the sensitivity of alignment of an edge-emitting diode laser to an optical fiber in applications such as telecom transmitters, thereby potentially reducing manufacturing costs. It has been reported that increasing fiber numerical aperture (NA) can be achieved by forming a hemispherical lenslet on the tip of the fiber by thermal melting and that the variation of acceptance angle with the lenslet radius of curvature may be estimated from the following relationship [12]

$$q(h) = \text{asin}(n_1 \cdot \sin(\text{asin}(h)) + \text{acos}(\tfrac{n_2}{n_1})) - \text{asin}(h) \quad (1)$$

where q is defined as

$$h = \frac{d}{2r} \quad (2)$$

By selecting typical telecommunication fiber values for core diameter (**d**), core index ($\mathbf{n_1}$), and cladding index ($\mathbf{n_2}$), respectively, the variation of fiber half-angle of acceptance with microlens radius of curvature (ROC) **r** may be plotted as in Figure 5. These data indicate that the magnitude of the increase in fiber acceptance angle with a hemispherical microlens on its tip with index of refraction identical to that of the core rises sharply as the radius of curvature of the printed lenslet is decreased, suggesting that at least a six-fold increase in angle could be achieved with a microlens diameter of 30 μm (15 μm ROC).

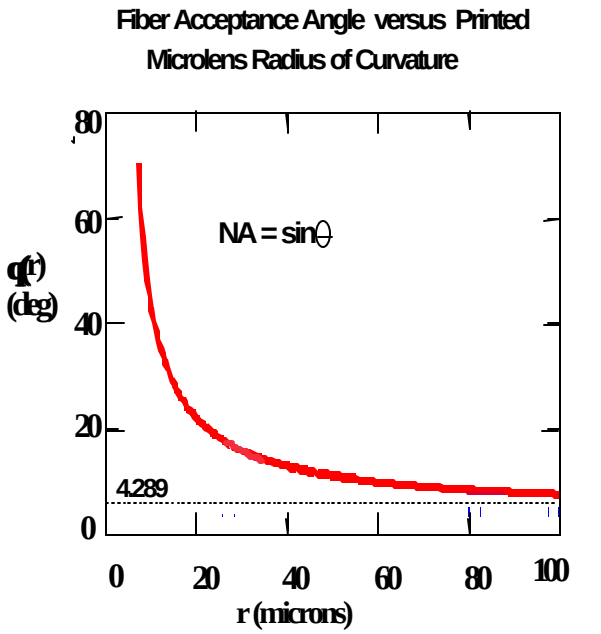

Figure 5. Half-acceptance angle q of a lensed fiber as a function of lenslet radius curvature r (in microns), when the telecom fiber core diameter is fixed at 8 micron. Index of core and cladding are 1.4616 and 1.4571 respectively, and the angle without a lenslet is 4.289.

We have previously shown that microlenses may be printed with differing radii of curvature onto the tips of multimode optical fibers so as to increase their acceptance angles of light from diode laser sources by at least a factor of three.[5] In the multimode fiber case the outer edge of the fiber cladding defines the diameter of the printed lens, so alignment of printing axis to fiber tip is not a critical issue, and the radius of curvature may be increased (within limits determined by surface tension) by increasing the number of droplets of deposited optical fluid.

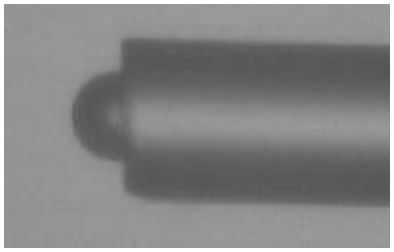

Figure 6. 70 μm diameter microlens printed onto the tip of a single-mode telecom fiber with cladding outside diameter of 125 μm (fiber courtesy of Corning).

To achieve similar acceptance angle increases in single-mode fibers is a more challenging proposition, because it requires placement of a much smaller, faster microlens at the center of the fiber tip. An example of a hemispherical microlens microjet printed onto the end of a single mode fiber of the configuration of Figure 5 is given in the photograph of Figure 6, where the lenslet diameter of 70 μm was achieved by depositing and UV-curing one 50 μm diameter droplet of optical epoxy, after applying a low-wet coating to the tip of the fiber. Alignment of the

Figure 7. Profile view of 65 μm diameter hemispherical microlenses printed onto the tips of single-mode fibers within a fiber array (fiber array courtesy of Radiant Research Inc.).

microlens to the fiber core within about 5 :m was achieved with a visual targeting system. Another example is shown in Figure 7, where 65 :m diameter microlenses were printed at the fiber positions of a linear array of single-mode fibers. In both cases precision of alignment of the printed microlens to the fiber core is the most challenging part of the process.

In the coupling of edge-emitting diode lasers into optical fibers the primary quantity of interest is the coupling energy efficiency, rather than fiber acceptance angle per say. The source-to-fiber coupling efficiency via a hemispherical microlens printed on top of a single-mode fiber is given by the well known overlap integral:

$$0 = \frac{\left|\iint \Psi_v \Psi_f^{**} dxdy\right|^2}{\iint |\Psi_v|^2 dxdy \iint |\Psi_f|^2 dxdy} \qquad (3)$$

where Q_v is the field of the fundamental mode of the single mode fiber, and Q_f the field of the laser diode transformed by the hemispherical microlens printed at the end of the fiber. An efficient numerical analysis for the energy coupling efficiency may be performed from Equation (3) by employing ABCD matrix for the refraction of paraxial rays by a hemispherical lens.[13] Using the corresponding analytical expression, we may calculate the coupling efficiency as a function of printed microlens radius of curvature, as shown in Figure 8, assuming: a 1550 nm wavelength for fiber and diode laser; fiber step index of 1.4514/1.4469, with core and cladding diameters of 9.3 :m and 125 :m, respectively; diode laser emitter dimensions of 0.843 :m x 0.857 :m; and printed microlens refractive index of 1.52. Comparing the curves of Figures 5 and 8, it can be seen that coupling efficiency increases at a much slower rate than fiber acceptance angle with decreasing lenslet radius, suggesting that a lenslet as small as 14 :m in diameter (ROC=7 :m) would be required to achieve the maximum predicted value of 6X increase in coupling efficiency (above the ~10-15% level obtained for a bare fiber which is perfectly aligned with the fiber core). However, a coupling efficiency increase of a factor of two should be obtainable by printing a 30-40 :m diameter lenslet on such a fiber. For the optimal, 14 :m diameter microlens, one can also calculate coupling efficiency as a function of misalignment distance between fiber and microlens axes, as indicated in Figure 9. In this case it can be seen that a misalignment greater than a couple of microns would begin to degrade significantly the efficiency gains obtained with the microlens.

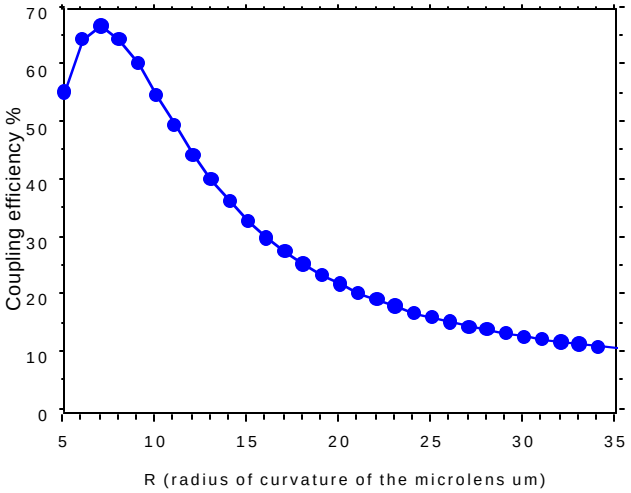

Figure 8. Efficiency of coupling (%) of energy from an edge-emitting diode laser into a single-mode optical fiber as a function of microlens radius of curvature (in microns).

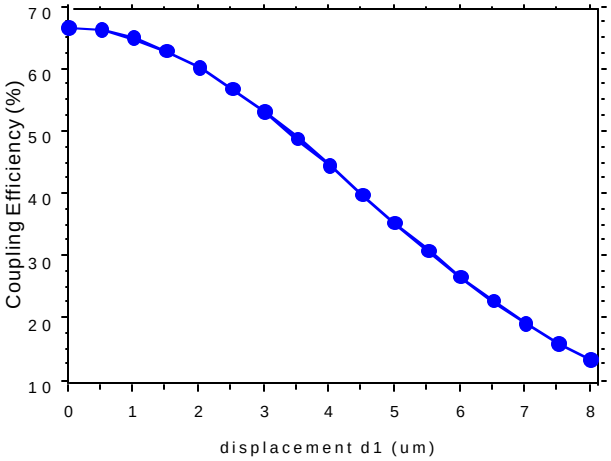

Figure 9. Efficiency of coupling (%) of energy from an edge-emitting diode laser into a single-mode optical fiber with a printed 14 :m diameter microlens as a function of displacement of the microlens from the fiber core axis (in microns).

4.2 Collimating fiber output

Collimation of the output beam of a single-mode optical fiber may also be achieved by printing a microlens onto its tip, but the geometry required is quite different from that needed to increase fiber NA. Ray trace modeling indicates that collimation requires a much larger microlens which is offset longitudinally from the tip by the lenslet focal length. As a first-cut approach to achieving collimation with a printed microlens we utilized a quartz collet on the end of the fiber to obtain the

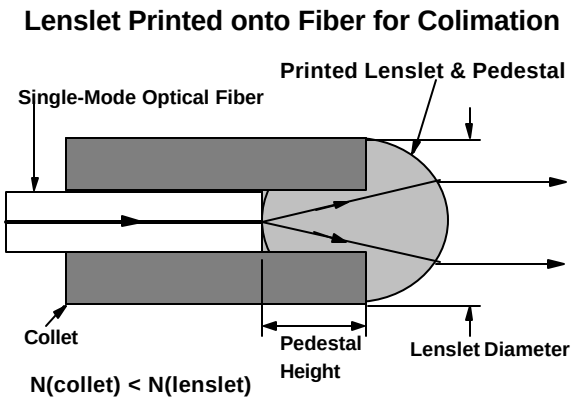

Figure 10. Geometry for collimating output of a single-mode optical fiber with a printed microlens.

requisite geometry, as illustrated schematically in Figure 10. The ID and OD of these 5 mm long collets matched the fiber OD and targeted lenslet diameter, respectively. Quartz was the collet material of choice because it has a lower index of refraction than the optical material used to print the microlenses, and would, therefor provide some wave-guiding advantages between the tip of the fiber and the entrance side of the lenslet. The fabrication procedure consisted of sliding this collet over the end of a fiber and gluing it into place, with the collet extending beyond the end of the fiber by the requisite lenslet offset distance. After mounting this "cup" assembly vertically and aligning it to the print axis, 50 μm droplets of optical epoxy were microjetted into the cup to fill it to the top of the collet and build a convex lenslet surface of optimal radius of curvature on the top. As in the case of multimode fiber printing the outside edge of the collet defined the printed microlens diameter, so the radius of curvature could be varied over a significant range by varying the total number of droplets of optical material. A photograph of a 1550 nm fiber with collet and printed microlens is shown in Figure 11.

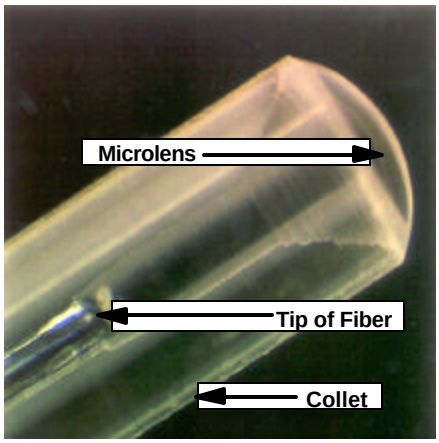

Figure 11. Microlens printed into and onto quartz collet attached to a single-mode optical fiber, per geometry of Fig. 10, in order to achieve collimation of fiber output beam (photo courtesy of Nortel Networks).

5. ARRAYS OF SENSOR ELEMENTS PRINTED ONTO OPTICAL IMAGING FIBERS

Another potentially significant application of microjet technology is fabrication of multi-functional fiber optic bio-chemical sensors, with potential use in clinical diagnosis [14], manufacturing process control, environmental monitoring, etc. If the UV-curing optical epoxies are adjusted to provide enhanced porosity over the formulations used for microlens printing and doped with biochemical indicators, they may be printed into patterns of sensor elements onto the tips of imaging fiber bundles, providing a sensor configuration as exemplified by the photographs of Figure 12.

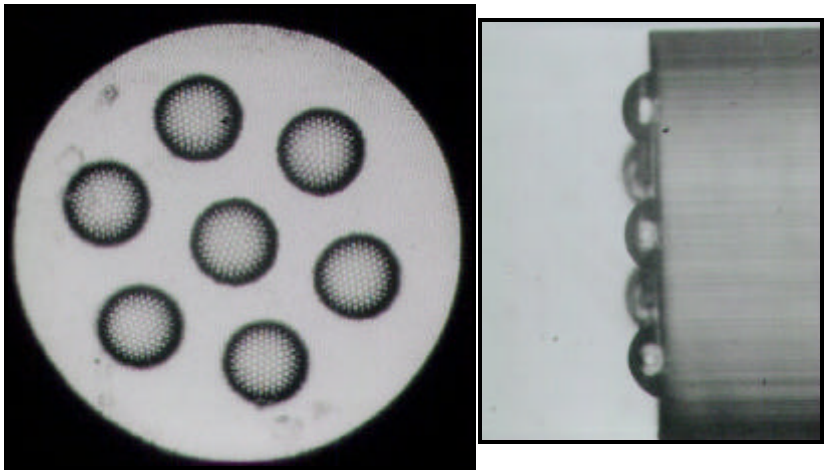

Figure 12. Array of 80 μm diameter hemispherical indicator elements printed onto 480 μm diameter fiber-optic bundle, shown from the top (left) and in profile (right), fluorescing under UV-illumination (fiber bundle courtesy of B. Coleston Jr. of Lawrence Livermore National Laboratories).

Biochemical fiber optic sensors in use today typically consist of an indicator chemistry attached to a single fiber, where the indicator chemistry is designed to change its optical properties (e.g., fluorescence or absorption) quantitatively in response to a target ligand under illumination of a suitable wavelength. The absorption or re-emission of the illuminating radiation in the form of fluorescence is monitored via photosensitive detectors, and a separate sensor is required for each target ligand.

Multi-functional array sensors have been fabricated previously with fiber imaging bundles using a series of steps to "grow" sequentially indicator elements by masking the end of the fiber and UV-curing each element out of different polymeric solutions[15], but poor uniformity and reproducibility of indicator element geometries have required calibration of each fiber and has limited their use.

The unique opportunity provided by microjet printing technology in this arena is the reproducible fabrication of large numbers of uniformly sized sensor elements consisting of different indicator chemistries on the same optical fiber bundle, in order to provide multi-functionality in a single sensor, using spatial and spectral filtering in the detector system. Initial characterization of fluorescing intensities from the seven elements printed with the same material on the fiber of Figure 12 have shown an element-to-element variation of less than 5%.[14] Utilizing multiple print heads with differing indicator chemistries, such multi-functional fiber-optical array sensors could be manufactured with microjet printing technology at very high throughput rates and low materials costs.

6. PRINTING OF AGRIN MICROLENSES

Cylindrical lenses having radial indexes of refraction gradients (RGRIN), with diameter ranging from about 60 ：m in gradient-index, multi-mode optical fibers[16] to about 10 mm in gradient index rod lenses[17], are fabricated by ion inter-diffusion in glass rods and are widely used in light collimation applications. Similarly, plano/convex macrolenses with axial index of refraction gradients (AGRIN), made by stacking, fusing and coring glass plates having differing indexes of refraction, then machining a hemispherical surface,[18] can produce many-fold reductions in focal spot sizes compared to homogeneous lenses of the same geometry.[19] However, there have not yet been fabricated, to our knowledge, stand-alone microlenses having refractive index gradients, in either glass or optical plastic.

Microjet printing would seem to offer a unique capability for inexpensive fabrication of gradient index microlenses of several configurations and for increasing performance significantly. For example, ray-trace modeling has indicated that an axial index gradient of only 0.01 in a hemispherical lenslet with 50 ：m sag could potentially provide a 50-fold reduction in focused spot size and a 25-fold increase in Strehl ratio (the ratio of the area under the modulation transfer function curve to that of an ideal, aberration-free lens) over a homogeneous lenslet of identical geometry, as shown in Figure 13.

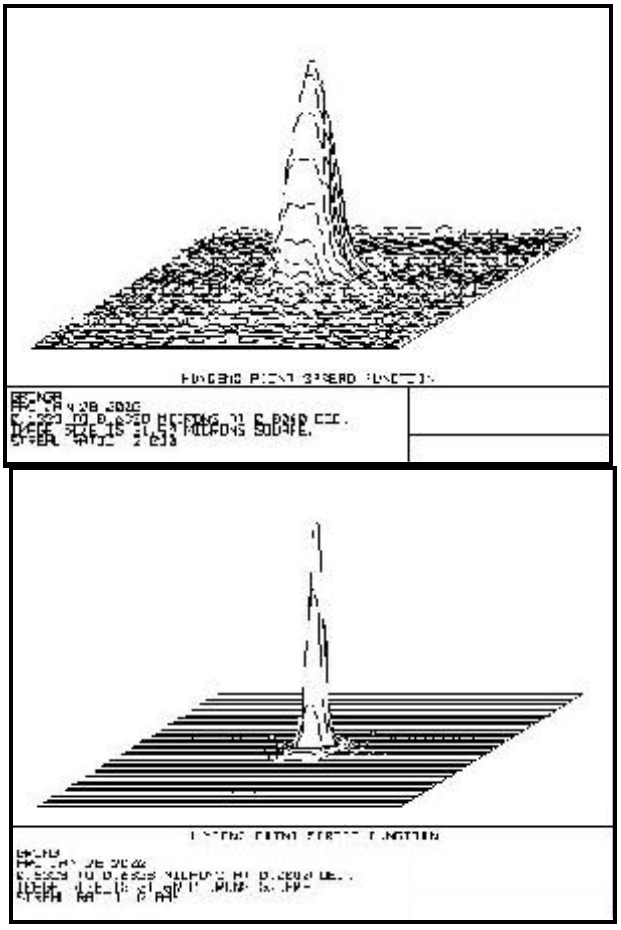

Figure 13. Comparison of calculated point spread functions for hemispherical microlens with 50 ：m sag both without (top) and with an axial index gradient of 0.01, which indicates a 25-fold increase in Strehl ratio provided by the index gradient

The process which we are starting to develop for microjet printing of microlenses with axial index gradients is illustrated conceptually in Figure 14. It utilizes a dual print head system, such as that pictured in Figure 15, to deposit sequentially two optical epoxies of differing refractive index at the same location, in order to build an index gradient in the vertical direction. The relative volumes of the two materials and the time allowed for inter-diffusion prior to solidification are process parameters which may be adjusted to maximize the axial component of the index gradient and its smoothness. The objective in developing two optical formulations for this application will be to maximize the spread in refractive index without sacrificing miscibility and microjetability.

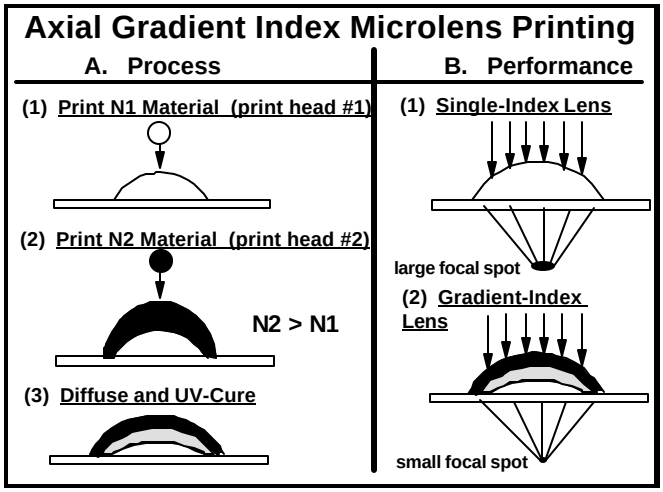

Figure 14. Proposed process (A) and desired performance (B) for microjet printing of axial gradient index of refraction microlenses.

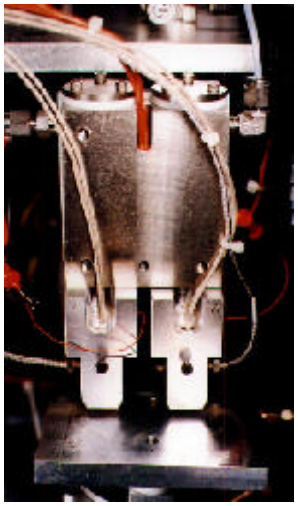

Figure 15. Dual print head system for two-fluid printing

Figure 16. Simulated AGRIN microlens, 300 ：m in diameter, printed by depositing fluorescing optical epoxy onto a prior deposition of non-fluorescing epoxy, viewed in profile under UV-irradiation.

The concept of this approach was tested by using two versions of the same optical material - one with and one without a fluoresceine dopant. Here the undoped material was deposited first, then the print head was translated to enable deposition of the second, fluorescing material at the same location. After an inter-diffusion time of 1 min, the composite structure was cured by UV-irradiation. The axial (bottom-to-top) fluorescein compositional gradient created in this hemispherical microlens can be seen under UV-illumination in the profile photograph of Figure 16, where the color changes from dark to light from the substrate plane to the apex of the lenslet.

7. CONCLUSIONS

We have argued that the microjet printing method of micro-optics has the general potential for reducing costs and enhancing assembly process integration in optoelectronics manufacturing. In particular, it offers unique benefits and is currently being employed in the fabrication of arrays of durable, low f/#, refractive, microlenses arrays for development of advanced VLSI smart-pixel datacom switches. Modeling data suggest that this “Optics-Jet” technology could be utilized to advantage in increasing coupling efficiency between edge-emitting diode lasers and single-mode optical fibers and in collimating single-mode fiber output beams, and we have built some fibers with printed microlenses for future testing to verify these models. Additional potentially significant applications for which microjet printing offers truly unique capabilities, which we have just begun to investigate, include the fabrication of multi-functional, fiber-optical biochemical sensors and microlenses with gradient indexes of refraction.

Future development efforts for this “Optics-Jet” technology will include: obtaining data for microlenses printed onto single-mode optical fibers; further improvement of microlens accuracy of placement; reduction in the minimum element dimension which can be printed with high accuracy; and fabrication & testing for performance of gradient index microlenses and array-on-fiber-based biochemical sensors.

8. ACKNOWLEDGMENTS

The underlying foundations and various components of this work have been supported in part by DARPA, the U.S. Army Research Office, the U.S. Air Force Phillips Lab, Honeywell, Nortel Networks, and Lawrence Livermore National Laboratories. Outside collaborators include Allen Cox and Yue Liu of Honeywell, Larry Marcanti and Michael Lovelady of Nortel Networks, and Bill Coleston Jr. of LLNL. Additional contributors within MicroFab include Hans-Jochen Trost and Rick Hoenigman. To all we express thanks.

9. REFERENCES

1. W.R. Cox, D.J. Hayes, T. Chen and D.W. Ussery, “Fabrication of micro-optics by micro-jet printing,” *SPIE Proceedings* **2383**, pp.110-115, 1995.
2. W.R. Cox, D.J. Hayes, T. Chen, H-J. Trost, M.E. Grove, R.F. Hoenigman and D.L. MacFarlane, “Low cost optical interconnects by micro-jet printing,” *IMAPS International Journal of Microcircuits & Electronic Packaging* **20**, No. 2, pp.89-95, 1997.
3. B.P. Kenworth, D.J. Corazza, J.N. McMullin and L. Mabbott, “Single-step fabrication of refractive microlens arrays,” *Applied Optics* **36**, No. 10, pp. 2198-2202, 1997.
4. D. Daly, R.F. Stevens, M.C. Hutley and N. Davies, “The manufacture of microlenses by melting photo-resist,” *Measurement Science & Technology* **1**, pp. 759-766, 1990.
5. W.R. Cox, T. Chen, D. Ussery, D.J. Hayes, J.A. Tatum and D.L. MacFarlane, “Microjetted lenslet-tipped fibers,” *Optics Communications* **123**, pp. 492-496, 1996.

6. V. Baukens, A. Goulet, H. Thienpont, I. Veretennicoff, W.R. Cox and C. Guan, "GRIN-lens based optical interconnection systems for planes of micro-emitters and detectors: Microlens arrays improve transmission efficiency," *OSA Diffractive Optics and Micro-Optics Topical Meeting*, Kailua-Kona, Hawaii, June, 1998.

7. D.B. Wallace, "A method of characteristics model of a drop-on-demand ink-Jet device using an integral drop formation method," *ASME Publication* **89-WA**/FE-4, December, 1989.

8. W.T. Pimbly, "Drop formation from a liquid jet: a linear one-dimensional analysis considered as a boundary value problem," *IBM journal of Research & Development* **29**, p.184, 1984.

9. W.R. Cox, T. Chen, C. Guan, D.J. Hayes, R.E. Hoenigman, B.T. Teipen and D.L. MacFarlane, "Micro-jet printing of refractive microlenses," *Proceedings, OSA Diffractive Optics and Micro-optics Topical Meeting*, paper #I-00002, Kailua-Kona, HW, June, 1998.

10. W.R. Cox, T. Chen, D.W. Ussery, D.J. Hayes, R.F. Hoenigman, D. L. MacFarlane and E. Rabonivich, "Microjet printing of anamorphic microlens arrays," *SPIE Proceedings* **2687**, pp. 89-98, 1996.

11. Y. Liu, et. al., "Component technology and system demonstration using smart pixel arrays based on integration of VCSEL/photodetector arrays and Si ASICs," *SPIE Photonics West Symposia*, paper CR76-05, January 25, 2000.

12. D. Kato, "Light coupling from a stripe-geometry GaAs diode laser into an optical fiber with spherical end," *J. Appl. Physics* **44**, No. 6, pp. 2756-2758, 1973.

13. S. Gangopadhyay, S.N. Sarkar, " Misalignment considerations in laser diode to single-mode fiber excitation via hemispherical lens on the fiber tip," J. Opt. Commun.**19,** No. 6, pp. 217-221, 1998.

14. B.W. Coleston Jr., D.M. Gutierrez, M.J. Everett, S.B. Brown, K.C. Langry, W.R. Cox, P.W. Johnson and J.N. Roe, "Intraoral fiber-optic-based diagnostics for periodontal disease," *SPIE Photonics West*, paper # 3911-03, January 25, 2000.

15. D.R. Walt and K.S. Bronk, "Thin-film fiber optic sensor array and apparatus for concurrent viewing and chemical sensing of a sample," *U.S. Patent 5,389,741*, 1994.

16. J. Hecht, "Fiberoptic communications: an optoelectronics driver," *Laser Focus World*, January, pp. 143-151, 1999.

17. T. Towe and S. Cai, "Gradient index lenses make light work of beam directing," *Laser Focus World*, October, pp. 93-96, 1999.

18. P.K. Manhart and R. Blankenbecler, "Fundamentals of macro axial gradient index optical design and engineering," *Optical Engineering*, vol. 36, No. 6, p.1607, 1997.

19. R.J. Pagano, K. Perkins and P.K. Manhart, "Axial gradient-index lenses come of age," *Laser Focus World*, pp.191-196, May, 1995.